



# Novel sulfonated polyimides containing multiple cyano groups for polymer electrolyte membranes

Yang Song<sup>a</sup>, Yinhua Jin<sup>a</sup>, Qiuju Liang<sup>a</sup>, Kechang Li<sup>a</sup>, Yunhe Zhang<sup>a</sup>, Wei Hu<sup>b</sup>,  
Zhenhua Jiang<sup>a</sup>, Baijun Liu<sup>a,\*</sup>

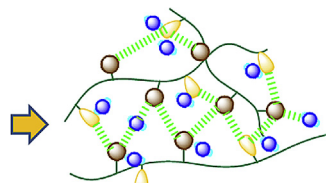
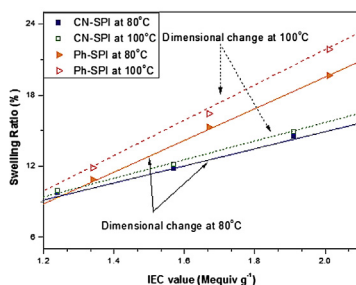
<sup>a</sup> College of Chemistry, Jilin University, 2699 Qianjin Street, Changchun 130012, PR China

<sup>b</sup> College of Chemical Engineering, Changchun University of Technology, 2055 Yan'an Street, Changchun 130012, PR China

## HIGHLIGHTS

- Novel multiple cyano-groups containing polyimides were prepared for PEM applications.
- The properties of the PEMs were carefully characterized.
- The cyano-functionalized SPIs exhibited some attractive properties.
- The CN-SPI membranes exhibited high proton conductivity and low swelling at 100 °C.

## GRAPHICAL ABSTRACT



The interactions between cyano and other polar groups could greatly improve the dimensional stability of the CN-SPI membranes at high evaluated temperature.

## ARTICLE INFO

### Article history:

Received 15 November 2012

Received in revised form

8 March 2013

Accepted 11 March 2013

Available online 26 March 2013

### Keywords:

Polyimides

Polymer electrolyte membranes

Fuel cells

Synthesis

Swelling

## ABSTRACT

Some multiple cyano groups functionalized sulfonated polyimides (CN-SPIs) are prepared derived from a novel CN-diamine monomer for the first time. Meanwhile, some similar SPIs but without cyano groups (Ph-SPIs) are prepared as counterparts for comparison purposes. Both chemical structure and properties of these SPIs are carefully characterized. At 100 °C, proton conductivities of some membranes could reach 0.138–0.146 S cm<sup>-1</sup>, which are comparative with Nafion. The methanol diffusion coefficients of the membranes are between 1.74 and 5.82 × 10<sup>-7</sup> cm<sup>2</sup> s<sup>-1</sup>, which are much more competitive than Nafion 117. It is of interest to find that cyano-functionalized SPIs could possess an excellent combination of low swelling, high proton conductivity and low methanol permeability.

© 2013 Elsevier B.V. All rights reserved.

## 1. Introduction

Fuel cells, including polymer electrolyte membrane fuel cells (PEMFCs) and direct methanol fuel cells (DMFCs), are widely regarded as promising clean future power sources for their attractive advantages such as high efficiency, environmental friendliness

and quiet operations [1–3]. Fuel cells have drawn extensive attention as potential energy devices in automotive, stationary and portable electronic applications [4–6]. Polymer electrolyte membranes (PEMs) play a dominate role in transporting protons between electrodes and preventing fuels crossover, thus becoming the most important component in PEMFCs [7–10]. Nowadays, most of commercial membranes are based on perfluorosulfonic acid polymers, such as DuPont's Nafion, which are widely used since they have attractive properties such as high proton conductivity, high chemical stability and excellent mechanical properties. However,

\* Corresponding author. Tel./fax: +86 431 8516 8022.

E-mail addresses: [liubj@jlu.edu.cn](mailto:liubj@jlu.edu.cn), [lbj7185@yahoo.com.cn](mailto:lbj7185@yahoo.com.cn) (B. Liu).

some drawbacks such as high cost, low operation temperature ( $\leq 80^\circ\text{C}$ ) and low methanol resistance may limit their wide applications in related areas [3,11,12].

Sulfonated poly(arylene ether ketone)s, sulfonated polyimides, phosphoric acid doped poly(benzimidazole)s and other acid-functionalized polyaromatics are promising candidates as alternative PEM materials due to their high thermal and chemical stability, high proton conductivity and low costs [13,14]. Among them, sulfonated polyimides (SPIs) have drawn some attention owing to their excellent properties such as heat resistance, chemical stability and good film-forming ability. Some useful structure–property relationships based on SPIs have been established by several research groups. For example, Mercier and his co-workers found that six-membered ring polyimides derived from 1,4,5,8-naphthalene tetracarboxylic dianhydride (NTDA) were more stable than common five-membered ring SPIs under fuel-cell conditions, which meant the possibility for polyimide-type polymers to be used for the PEMs [15,16]. Later, Watanabe claimed that some SPIs were stable for about 5000 h under fuel cell operating conditions [17]. Okamoto et al. indicated that NTDA-based SPIs with flexible ether linkages exhibited improved water stability and mechanical properties [18]. Watanabe and Miyatake even reported a SPI containing fluorenyl groups having a high proton conductivity of  $1.67\text{ S cm}^{-1}$  at  $120^\circ\text{C}$  under 100% relative humidity (RH) [19].

It is well known that the strong acidity of  $-(\text{CF}_2)_2-\text{SO}_3\text{H}$  pendants could endow Nafion with high proton conductivity, and high proton conductivity is crucial for the PEMs applied in fuel cell systems. In contrast, the high proton conductivity of polyaromatic-type PEMs will heavily depend on their high contents of  $-\text{SO}_3\text{H}$  groups [20–22]. These high ion-exchange capacity (IEC) values will cause the side effects, such as unacceptable dimensional changes and the loss of the mechanical integrity, especially at high humidity and high temperature [3,9].

In order to resolve these problems, several ways have been adopted. For example, Liu et al. reported some high-IEC sulfonated/carboxylated poly(aryl ether ketone)s, whose  $-\text{COOH}$  groups could be reacted with the  $-\text{OH}$  groups of poly(vinyl alcohol) to prepare crosslinked membranes [20]. Guo et al. prepared some molecule-enhanced blend PEMs through the acid–base interactions and they showed low-swelling and good methanol resistance [10,23]. Despite the obvious improvement on the dimensional stability, the complicated procedures need to be involved to build these cross-linkable or blending systems.

It is well known that polar cyano ( $-\text{CN}$ ) groups have large dipole moment and large polarizability, thus they can form stable complex through hydrogen bonds and strong intermolecular forces. In

addition, the cyano-containing polymers usually have strong interaction with the matrix, when they work as coatings [24–28]. These unique properties on the PEMs may be beneficial to dimensional stability and also to the integrity of the sandwiched structure membrane electrode assemblies (MEAs). In this study, as an attempt to find a new way to prepare low-swelling and high performance membrane materials, the multiple cyano-containing SPI-type PEMs have been prepared for the first time and the effects on the properties of the  $-\text{CN}$  groups have been revealed. Also, the properties including thermal and oxidative stabilities, water uptake and dimensional stability, methanol permeability and proton conductivity of both triple cyano groups-containing SPIs (CN-SPI) and the SPIs without cyano groups (Ph-SPI), have been studied thoroughly.

## 2. Experimental

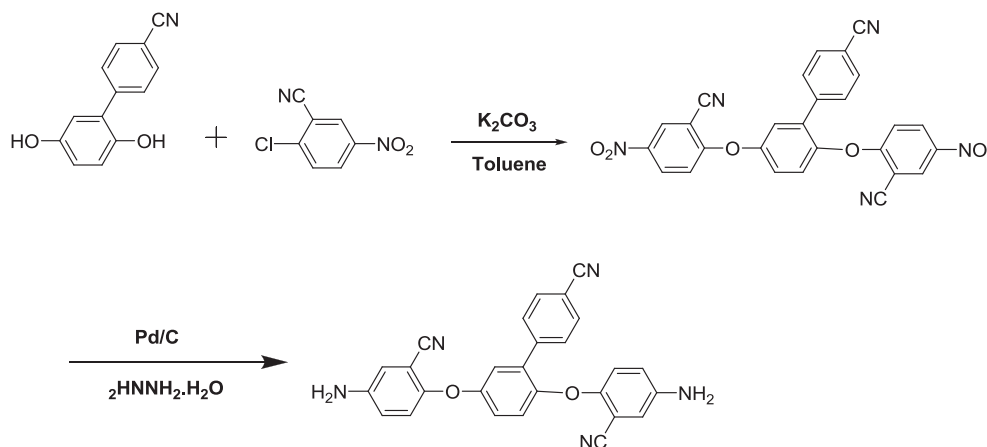
### 2.1. Chemicals and materials

3-Cyano-phenyl hydroquinone was synthesized in our lab according to a previous work [28]. 2-Chloro-5-nitrobenzonitrile (Shanghai Darui Finechem Ltd.), 4,4'-diamindodiphenyl ether (TCI), 1-chloro-4-nitrobenzene (Sigma–Aldrich) and 2,5-dihydroxybi phenyl (Sigma–Aldrich), triethylamine (Tianjin Chemical Reagent, China), *m*-cresol (Shanghai Chemical Reagent, China), benzoic acid (Tianjin Chemical Reagent, China) and fuming sulfuric acid ( $\text{SO}_3$  30%, Beijing Chemical Reagent, China) were used as received. Potassium carbonate (Beijing Chemical Reagent, China) was ground into fine powder and kept at  $120^\circ\text{C}$  prior to use. 1,4,5,8-Naphthalene tetracarboxylic dianhydride (NTDA) was purchased from Sigma–Aldrich, dried at  $160^\circ\text{C}$  in vacuo for 20 h before use. 4,4'-Diamindodiphenyl ether-2,2'-disulfonic acid (ODADS) was synthesized according to synthesis routines reported by Okamoto and his co-workers [18]. *N,N*-Dimethylformamide (DMF, Tianjin Chemical Reagent, China), dimethyl sulfoxide (DMSO, Tianjin Chemical Reagent, China), acetone (Beijing Chemical Reagent, China) and toluene (Beijing Chemical Reagent) were used as solvents and azeotropic reagent separately.

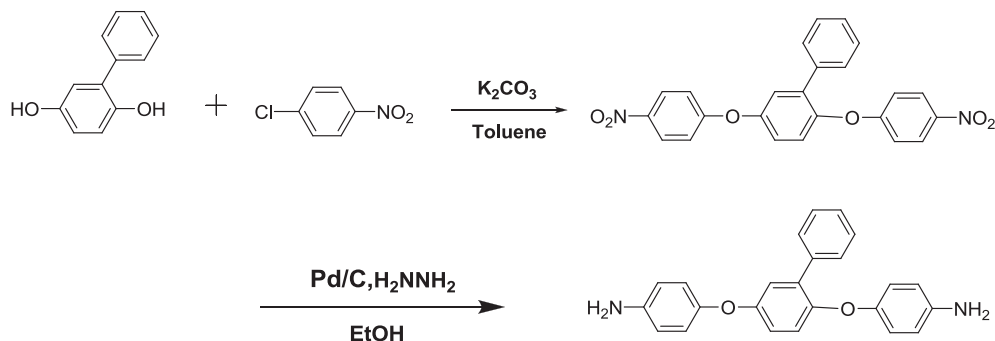
### 2.2. Synthesis of the monomers (Schemes 1 and 2)

#### 2.2.1. Synthesis of 2,5-bis(4-nitro-2-cyanophenoxy)-1-cyano-benzene(CNDN)

Into a 250 mL three-neck flask equipped with a nitrogen inlet, a Dean–Stark Trap with condenser and a magnetic stirrer, were put 3.168 g (0.015 mol) of 3-cyano-phenyl hydroquinone, 5.751 g (0.0315 mol) of 2-chloro-5-nitrobenzonitrile and 2.3 g (0.017 mol)



**Scheme 1.** Synthesis of cyano containing diamine monomer (CNDN).



Scheme 2. Synthesis of non-cyano diamine monomer (BDA).

of  $\text{K}_2\text{CO}_3$ , *N,N*-Dimethylformamide (45 mL) and Toluene (10 mL) were added as solvent and azeotropic reagent separately. The mixture was refluxed at 130–135 °C for 2–3 h, and then a toluene/water mixture was removed. The system was refluxed without Dean–Stark Trap at 150 °C for another 3 h and poured into 200 mL of cold ethanol to obtain yellow solid. Crude product of dinitro monomer was washed in boiled deionized water for several times and then dried at 80 °C in an oven, a yellow product was obtained (yield 95%).

FTIR: 1025, 1080 ( $-\text{SO}_3\text{H}$ ); 1510 ( $-\text{NO}_2$ ); 2245 ( $-\text{CN}$ ).

$^1\text{H}$  NMR (DMSO- $d_6$ , ppm): 8.92 (s, 1H); 8.84 (s, 1H); 8.48 (d,  $J = 6.0$  Hz, 2H); 8.38 (d,  $J = 6.0$  Hz, 2H); 7.90 (d,  $J = 8.0$  Hz, 2H); 7.75 (d,  $J = 8.0$  Hz, 2H); 7.64 (d,  $J = 8.0$  Hz, 2H); 7.60 (s, 1H); 7.35 (d,  $J = 8.0$  Hz, 1H); 7.16 (d,  $J = 8.0$  Hz, 1H).

#### 2.2.2. Synthesis of 2,5-bis(4-amino-2-cyanophenoxy)-1-cyanobenzene (CNDA)

CNDN (5.03 g, 0.01 mol), 0.4 g 10% Pd/C and 15 mL hydrazine hydrate were added into a 250 mL three-necked flask equipped with a nitrogen inlet with a dropping funnel, a condenser and a magnetic stirrer. 100 mL ethanol was added as solvent. The mixture was refluxed with stirring for 4 h, after hot filtration, the yellow filtrate was poured into 300 g ice and white precipitation was gained by filtration. The crude product was then recrystallized by aqueous ethanol and dried in vacuum at 80 °C over night. Off-white product was obtained (yield 75%).

FTIR: 3450 ( $-\text{NH}_2$ ); 2245 ( $-\text{CN}$ ).

$^1\text{H}$  NMR (DMSO- $d_6$ , ppm): 7.90 (d,  $J = 10.0$  Hz, 2H); 7.75 (d,  $J = 10.0$  Hz, 2H); 7.15 (s, 1H); 7.04 (d,  $J = 6.0$  Hz, 2H); 6.98 (d,  $J = 6.0$  Hz, 2H); 6.92 (d,  $J = 8.0$  Hz, 2H); 6.85 (d,  $J = 8.0$  Hz, 2H); 6.80 (s, 2H).

#### 2.2.3. Synthesis of 2,5-bis(4-aminophenoxy)biphenyl (BDA)

The BDA monomer was synthesized using a similar procedure to CNDA (yield 78%).

FTIR: 3350 ( $-\text{NH}_2$ ); 1250 ( $\text{C}-\text{O}$ ).

$^1\text{H}$  NMR (DMSO- $d_6$ , ppm): 7.55 (d,  $J = 8.0$  Hz, 2H); 7.36 (d,  $J = 8.0$  Hz, 2H); 7.28 (t,  $J_1 = 6.0$  Hz,  $J_2 = 6.0$  Hz, 1H); 6.98 (s, 1H); 6.89 (d,  $J = 8.0$  Hz, 2H); 6.87 (d,  $J = 8.0$  Hz, 1H); 6.85 (d,  $J = 8.0$  Hz, 1H); 6.75 (d,  $J = 8.0$  Hz, 2H); 6.70 (d,  $J = 8.0$  Hz, 2H); 6.63 (d,  $J = 8.0$  Hz, 2H).

#### 2.3. Synthesis of the CN-SPIs (Scheme 3)

ODADS (0.721 g, 2 mmol), triethylamine (0.48 g, 4.8 mmol) and *m*-cresol (10 mL) were placed into a 50 mL three-neck flask equipped with a nitrogen inlet, a mechanical stirrer and a drying tube. After the mixture were totally dissolved at 50 °C, 0.888 g (2 mmol) of CNDA, 1.072 g (4 mmol) of NTDA and 0.68 g (5.6 mmol) of benzoic acid were added and the mixture were

stirred at 80 °C for 4 h. The mixture was heated to 175 °C in an oil bath for 15 h and then the temperature was increased to 195 °C for another 3 h. After cooling to 100 °C, an additional 10 mL of *m*-cresol was added to dilute the highly viscous solution. It was poured into 200 mL of acetone to yield dark brown fiber-like product (CN-SPI-2). It was filtrated, washed with acetone for several times and dried in vacuo.

FTIR (CN-SPI): 1025, 1080 ( $-\text{SO}_3\text{H}$ ); 1350 ( $\text{C}-\text{N}$ ); 1675, 1720 ( $\text{C}=\text{O}$ ); 2245 ( $-\text{CN}$ ).

$^1\text{H}$  NMR (CN-SPI-2 as example, DMSO- $d_6$ , ppm): 8.70 (s, 8H); 8.10 (s, 2H); 8.04 (s, 2H); 7.94 (d,  $J = 6.0$  Hz, 2H); 7.90 (d,  $J = 8.0$  Hz, 2H); 7.86 (d,  $J = 8.0$  Hz, 2H); 7.72 (d,  $J = 6.0$  Hz, 2H); 7.66 (d,  $J = 6.0$  Hz, 1H); 7.62 (s, 1H); 7.45 (d,  $J = 8.0$  Hz, 2H); 7.38 (d,  $J = 8.0$  Hz, 1H); 7.25 (d,  $J = 8.0$  Hz, 2H).

Using the same procedure, CN-SPI-1 (IEC = 1.24 mequiv  $\text{g}^{-1}$ ), CN-SPI-3 (IEC = 1.91 mequiv  $\text{g}^{-1}$ ), CN-SPI-4 (IEC = 2.14 mequiv  $\text{g}^{-1}$ ) were synthesized through adjusting the feed ratios of the monomers.

#### 2.4. Synthesis of the SPIs without $-\text{CN}$ groups (Scheme 3)

The corresponding SPIs with similar chemical structure and without  $-\text{CN}$  groups were also synthesized using the similar synthetic procedures, and BDA was used to replace CNDA. They were named as Ph-SPI-1 (IEC = 1.11 mequiv  $\text{g}^{-1}$ ), Ph-SPI-2 (IEC = 1.34 mequiv  $\text{g}^{-1}$ ), Ph-SPI-3 (IEC = 1.67 mequiv  $\text{g}^{-1}$ ) and Ph-SPI-4 (IEC = 2.01 mequiv  $\text{g}^{-1}$ ). The synthesis routine is shown in Scheme 3.

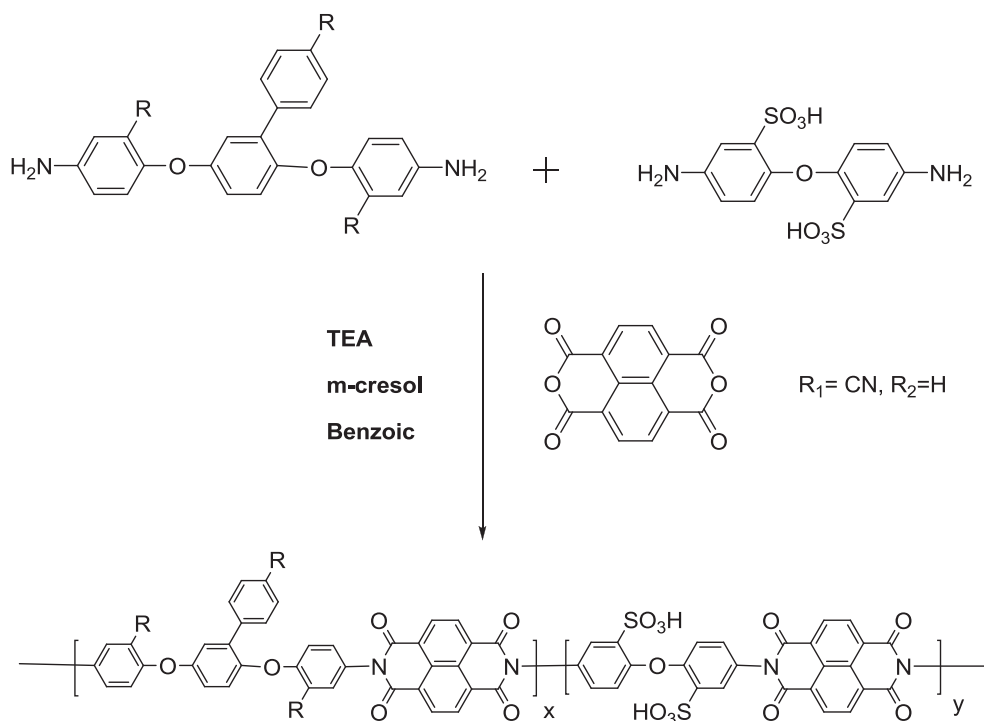
The FTIR and NMR results of Ph-SPI-3 were given as example.

FTIR (Ph-SPI): 1025, 1080 ( $-\text{SO}_3\text{H}$ ); 1350 ( $\text{C}-\text{N}$ ); 1675, 1720 ( $\text{C}=\text{O}$ ).

$^1\text{H}$  NMR (DMSO- $d_6$ , ppm): 8.70 (s, 8H); 7.92 (s, 2H); 7.65 (d,  $J = 6.0$  Hz, 2H); 7.55 (d,  $J = 8.0$  Hz, 4H); 7.50 (s, 1H); 7.45 (d,  $J = 8.0$  Hz, 2H); 7.42 (d,  $J = 6.0$  Hz, 2H); 7.39 (t,  $J_1 = 6.0$  Hz,  $J_2 = 6.0$  Hz, 1H); 7.30 (d,  $J = 8.0$  Hz, 4H); 7.28 (d,  $J = 8.0$  Hz, 1H); 7.22 (d,  $J = 8.0$  Hz, 1H); 7.12 (d,  $J = 6.0$  Hz, 2H).

#### 2.5. Membrane preparation

SPI polymers (0.7 g) were completely dissolved in 8 mL (for Ph-SPI series) and 10 mL (for CN-SPI series) of DMSO, respectively. The SPI solution was filtrated using fiber filter clothes to provide clean solution, and then the filtration was cast onto a 8 × 8 cm glass plate. After drying at 60 °C for 10 h and then treating in vacuum at 100 °C for another 10 h, flexible, tough and homogeneous membranes were obtained. The films were immersed in a 2 M  $\text{H}_2\text{SO}_4$  at room temperature for 12 h to convert them into acid form. Acidified films were washed with deionized water till their pH value was approached to 7. The thickness of the membranes was in the range of 60–100  $\mu\text{m}$ .



**Scheme 3.** Synthesis of cyano containing SPI (CN-SPI-X) and non-cyano containing SPI (Ph-SPI-X).

## 2.6. Characterization

### 2.6.1. FTIR, NMR and viscosity measurements

FTIR spectra were obtained on a Nicolet Impact 410 Fourier-transform infrared spectrometer.  $^1\text{H}$  NMR (500 MHz) spectra were recorded on a Bruker 510 spectrometer using  $\text{DMSO}-d_6$  as solvent. Viscosities of the sulfonated polyimides were measured using a thermostatically controlled Ubbelohde Viscometer with polymer concentrations of  $0.5 \text{ g dL}^{-1}$  in DMSO.

### 2.6.2. Water uptake and swelling ratio measurements

Film samples were cut into rectangle shapes with the dimension of  $10 \text{ mm} \times 30 \text{ mm}$  and dried at  $120^\circ\text{C}$  in vacuum for 24 h, and then the lengths and weights of the candidate samples were accurately recorded. Samples were immersed in deionized water to reach equilibrium at desired temperatures. The water on the surface was removed with a paper towel, and weights and lengths of the films were quickly measured. The water uptake of a membrane was calculated from following relations:

$$\text{Water uptake}(\%) = \frac{W_{\text{wet}} - W_{\text{dry}}}{W_{\text{dry}}} \times 100$$

where  $W_{\text{wet}}$  and  $W_{\text{dry}}$  were weights of wet and dry membrane samples, respectively.

The swelling ratio was calculated from the change of film length using the following equation:

$$\text{Swelling ratio}(\%) = \frac{L_{\text{wet}} - L_{\text{dry}}}{L_{\text{dry}}} \times 100$$

where  $L_{\text{wet}}$  and  $L_{\text{dry}}$  represented the lengths of wet and dry membrane samples, respectively.

### 2.6.3. Ion-exchange capacity (IEC) of membranes

The IEC values of sulfonated films were determined by classical titration. Membrane samples (about 60 mg) were immersed in

25 mL 2 M NaCl solution for at least 48 h to liberate  $\text{H}^+$  ions which were replaced by  $\text{Na}^+$  ions from membranes. The exchanged protons within the solutions were titrated with 5 mM NaOH aqueous solution and phenolphthalein was used as an indicator. Several measurements were carried out until constant values were obtained. IEC values were calculated via the following equation:

$$\text{IEC} = \frac{\text{consumed NaOH}(\text{ml}) \times \text{molarity of NaOH}}{\text{weight of dried membrane}} (\text{mequiv g}^{-1})$$

### 2.6.4. Thermal and oxidative stability

Differential scanning calorimeter (DSC) was performed on a Mettler Toledo DSC 821e instrument from  $80^\circ\text{C}$  to  $200^\circ\text{C}$  at a heating rate of  $20^\circ\text{C min}^{-1}$  under nitrogen atmosphere at a constant flow of  $200 \text{ mL min}^{-1}$ . Thermal gravimetric analyses (TGA) were determined by a Netzsch Sta 449c instrument. Membrane samples were dried in vacuum before measurement, and then were kept in the TGA furnace at  $120^\circ\text{C}$  under nitrogen atmosphere for 20 min. After that, films were reheated to  $800^\circ\text{C}$  at a heating rate of  $10^\circ\text{C min}^{-1}$ . The temperature at 5% and 10% weight loss were recorded for each sample.

A small piece of membrane sample was soaked in Fenton's reagent (3%  $\text{H}_2\text{O}_2$  containing 2 ppm  $\text{FeSO}_4$ ) at  $80^\circ\text{C}$ , and oxidative stability was evaluated by recording the dissolution time ( $t$ ) of the polymer membranes and the retained weights of membranes after treating in Fenton's reagent for 1 h.

### 2.6.5. Mechanical properties of membranes

The mechanical properties of membranes of dry membranes were measured at room temperature on SHIMADZU AG-1 KN at a strain rate of  $2 \text{ mm min}^{-1}$ . The size of samples was  $15 \text{ mm} \times 4 \text{ mm}$ . Wet state samples were treated by immersing them into deionized water for at least 48 h before test, and the measurement is similar to those of dry membrane samples.

### 2.6.6. Proton conductivity

Proton conductivity of the membranes was obtained by using an AC impedance spectroscopy (Solartron-1260/1287 impedance analyzer) with frequency range and oscillating voltage of 10–10<sup>7</sup> Hz, 50–500 mV. Membrane samples (5 cm × 1 cm) were placed into a four-point test cell comprising two outer gold wires that provided feed current to the sample and inner gold wires that were used to measure the voltage drops. The specimens were fully hydrated in deionized water for 24 h period to measurement, and the proton conductivity of films was measured at desired temperatures and the values were calculated via following equation:

$$\sigma = \frac{L}{R \times A}$$

where  $R$  was the membrane resistance,  $L$  was the distance between the electrodes and  $A$  was the cross-sectional area of membrane.

### 2.6.7. Methanol permeability

Methanol diffusion coefficient was determined by performing on a cell made up of two-half-chambers separated by the membrane being measured, which was fixed between two rubber washers. Aqueous methanol (100 mL, 10 mol L<sup>-1</sup>) was added to side (A) of the diffusion cell, and 100 mL of deionized water was placed in the other side (B). The liquids in both compartments were magnetically stirred to ensure solution uniformity. The methanol concentrations in B cell were investigated by using SHIMADZU GC-8A chromatograph. The methanol permeability coefficient was calculated via following formula.

$$C_B(t) = \frac{A}{V_B} \frac{DK}{L} C_A(t - t_0)$$

where  $A$ ,  $L$  and  $V_B$  were the diffusion area, membrane thickness, and the permeated water volume separately.  $C_B$  and  $C_A$  were methanol concentration in water compartment and methanol compartment, respectively.  $t_0$  was the time lag, and  $DK$  was the methanol diffusion coefficient.

## 3. Results and discussion

### 3.1. Preparation of the polymers

As an attempt of improving dimensional stability and mechanical properties of polymer electrolyte membranes, multiple cyano groups, which had highly polarity, would be introduced the backbones of SPI polymers. The synthetic strategies started from the synthesis of a triple cyano containing diamine monomer (CNDA), as shown in Scheme 1. Firstly, a novel dinitro compound, 2,5-bis(4-

**Table 1**  
Basic properties of copolymers.

Polymer	$\eta$ (dL g <sup>-1</sup> )	Td (°C)		IEC value (mequiv g <sup>-1</sup> )	
		5%	10%	Theoretical	Titration
CN-SPI-1	1.54	398.1	532.4	1.24	1.21
CN-SPI-2	1.29	386.7	509.1	1.57	1.53
CN-SPI-3	1.75	367.8	486.9	1.91	1.88
CN-SPI-4	1.48	360.2	413.4	2.14	2.06
Ph-SPI-1	1.03	450.3	549.6	1.11	1.08
Ph-SPI-2	0.93	417.8	541.9	1.34	1.26
Ph-SPI-3	0.78	369.8	443.6	1.67	1.62
Ph-SPI-4	0.85	357.8	424.7	2.01	1.98

$\eta$ : The viscosity of the polyimides measured by Ubbelohde Viscometer with polymer concentrations of 0.5 g dL<sup>-1</sup> in DMSO.

Td: The temperatures of 5% weight loss and 10% weight loss of polymers separately measured by TGA.

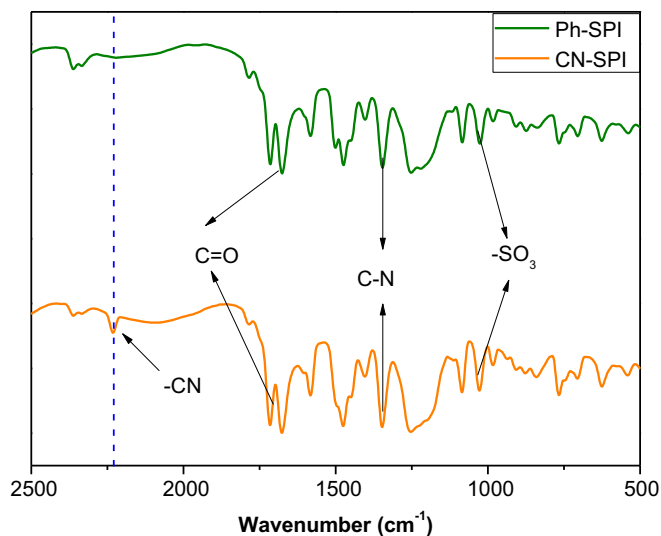


**Fig. 1.** FTIR spectra of CN-SPI-X and Ph-SPI-X polymers.

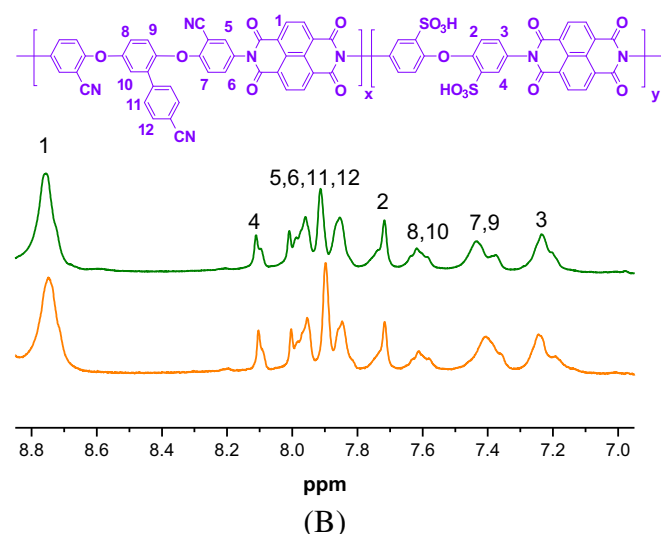
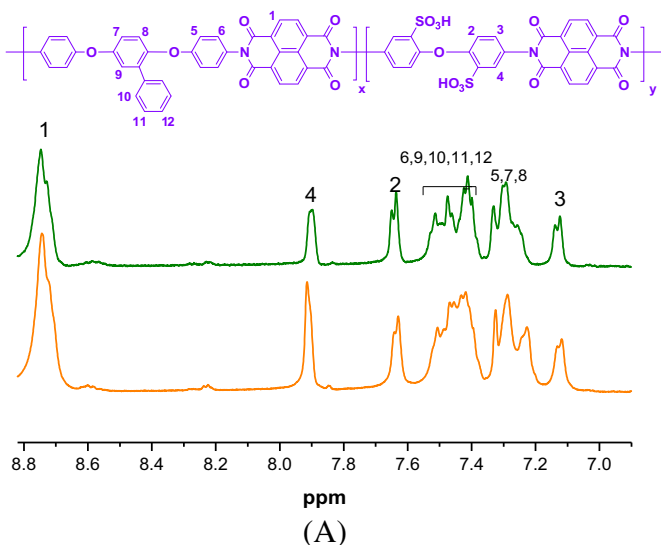


**Fig. 2.** <sup>1</sup>H NMR spectra of Ph-SPI-3 and -4 (A), CN-SPI-2 and -3 (B).

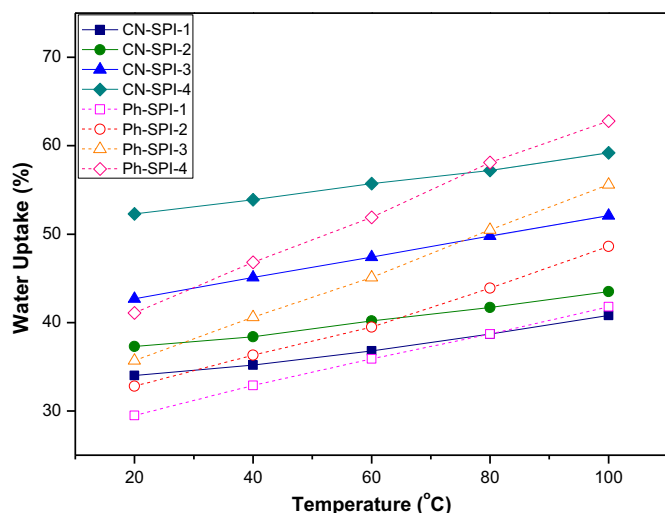
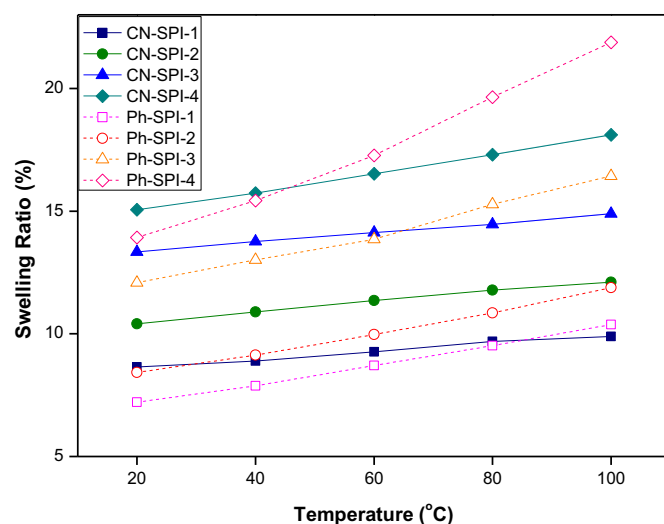
**Table 2**

Water uptake and swelling ratio of membranes.

Polymer	Water uptake (%)			Swelling ratio (%)		
	20 °C	80 °C	100 °C	20 °C	80 °C	100 °C
CN-SPI-1	34.1	38.7	40.8	8.65	9.69	9.89
CN-SPI-2	37.3	41.7	43.5	10.41	11.78	12.11
CN-SPI-3	42.7	49.8	52.1	13.34	14.46	14.89
CN-SPI-4	52.3	57.2	59.2	15.06	17.31	18.11
Ph-SPI-1	29.5	38.7	41.8	7.21	9.52	10.38
Ph-SPI-2	32.8	43.9	48.6	8.43	10.85	11.88
Ph-SPI-3	35.7	50.5	55.6	12.08	15.28	16.43
Ph-SPI-4	41.1	58.1	62.8	13.92	19.64	21.88

nitro-2-cyanophenoxy)-1-cyano-benzene, was synthesized via the aromatic nucleophilic substitution reaction from (3-cyano)phenylhydroquinone and 2-chloro-5-nitrobenzonitrile in the presence of  $K_2CO_3$ . Secondly, the diamine monomer, 2,5-bis(4-amino-2-cyano-phenoxy)-1-cyano-benzene (CNDA), was synthesized via a reduction of the dinitro-compound in the presence of  $Pt/H_2$  system. Another diamine having similar chemical structure, 2,5-bis(4-aminophenoxy)biphenyl [29], was synthesized using the same procedure (Scheme 2). Finally, triple cyano groups functionalized sulfonated polyimide copolymers (CN-SPIs) are synthesized through a “one pot” polymerization of CN-diamine, a presulfonated diamine and 1,4,5,8-naphthalenetetracarboxylic dianhydride (Scheme 3). Meanwhile, some similar SPIs but without cyano groups (Ph-SPIs) are prepared as counterparts for comparison purposes. The IEC values of the SPIs could be readily adjusted by changing the feed ratios of the CN-diamine/sulfonated diamine (or Ph-diamine/sulfonated diamine) monomers (Table 1).

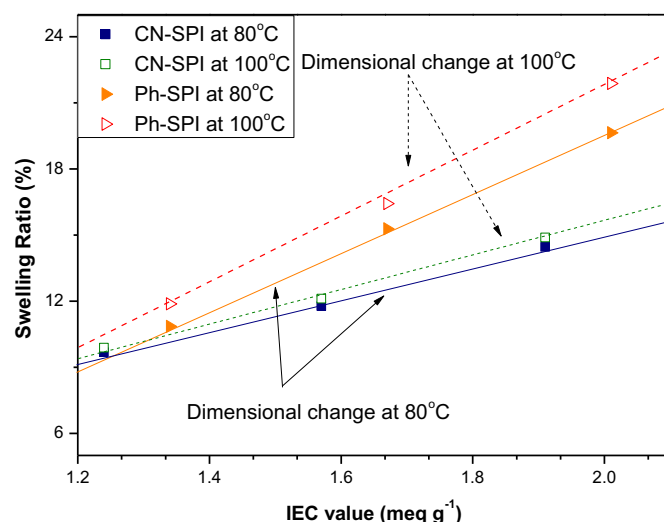
Structures of both monomers and polyimides were confirmed by FTIR and  $^1H$  NMR spectroscopy. Both dinitro and diamine monomers (CNDN and CNDA) exhibited an apparent vibration around  $2245\text{ cm}^{-1}$  was the signal of  $-CN$  groups. Meanwhile, stretching vibration of  $-NO_2$  group was at  $1510\text{ cm}^{-1}$  in CNDN monomers and vibration of  $-NH_2$  group was shown at around  $3450\text{ cm}^{-1}$  in DNDA monomers. In the  $^1H$  NMR spectra, all spectral signals were assigned to the protons of compound structures and clearly marked in the spectrum. FTIR and  $^1H$  NMR spectra of CN-SPI-Xs and Ph-SPI-Xs were shown in Fig. 1 and Fig. 2. In FTIR spectrum (non-sulfonated diamine versus ODADS feed ratio is 1:1), both SPI curves exhibited the symmetric, asymmetric vibration of  $C=O$  around  $1675$  and  $1720\text{ cm}^{-1}$ . The absorptions around  $1025$ ,  $1080\text{ cm}^{-1}$  were corresponded to the stretching vibration of  $-SO_3H$  groups, the vibration

**Fig. 3.** Water uptake of the membranes.**Fig. 4.** Swelling ratio of the membranes.

of  $C-N$  groups of the six-membered imide rings was near  $1350\text{ cm}^{-1}$ . CN-SPI showed an obvious signal at  $2240\text{ cm}^{-1}$ , indicating the vibration of  $-CN$  groups which cannot be found in Ph-SPI polymers.  $^1H$  NMR spectra of both series of polymers were run to confirm the structure of the polymers. Taking Ph-SPI-X as example (feed ratio of ODADS/BsDA = 1/1 X = and 1.5/1 separately), all H-signals were assigned to the protons and the proportion of signal peak area is reasonable to the feed ratio of polymers.

### 3.2. Water uptake and swelling ratio of the membranes

Water absorption, which is closely related to the IEC values and proton conductivity of membranes, plays a dominated role in evaluating the ultimate performance of PEM materials. Existence of water molecules in the sulfonated membranes will be greatly helpful for the transport of protons. However, over absorption of water destroys the dimensional stability of membranes, and the mechanical properties decrease dramatically by swelling [20]. In the fields of the PEM preparation, one of the trends nowadays is to synthesize low swelling materials even at high IEC levels.

**Fig. 5.** Dimensional change comparison between CN-SPI and Ph-SPI at the same IEC values at desired temperatures.

Different from some reported strategies, in which crosslinking or blending are involved, multi-cyano-groups functionalized SPIs (CN-SPI-X) were firstly synthesized in this study as an attempt to enhance the dimensional stability through the strong interactions of polar  $-\text{CN}$  groups. In order to the effects of the  $-\text{CN}$  groups on the performance, Ph-SPI-X polymers without  $-\text{CN}$  groups were prepared as counterparts.

Water uptakes of all the SPI membranes were evaluated and the results are shown in Table 2 and Fig. 3. Both CN-SPIs and Ph-SPIs showed increments of water absorption with the increase of the test temperature. However, it was interesting to observe, for each of the samples, the increasing range of the CN-SPIs series was much smaller with the increase of the test temperature. In addition, at the low test temperature, CN-SPIs series showed higher water uptakes than corresponding Ph-SPIs series at the similar IEC values. In contrast, at high temperature (above  $80^\circ\text{C}$ ), the water uptake values

of the Ph-SPIs series obviously exceeded their corresponding CN-SPIs ones. These results could be well explained by the existence of the abundant polar  $-\text{CN}$  groups on the CN-SPI backbones. As polar groups,  $-\text{CN}$  groups would show more hydrophilicity than nonpolar  $-\text{Ph}$  groups, leading to higher water uptake of CN-SPIs at low temperature. With the increase of the temperature, the water absorption ability of  $-\text{SO}_3\text{H}$  groups became dominant. Consequently, the strong interactions or hydrogen bonds of  $-\text{CN}$  and  $-\text{CN}$ ,  $-\text{CN}$  and  $-\text{SO}_3\text{H}$ , and  $-\text{CN}$  and other polar groups, may obviously restrict the dimension change of the membranes. The swelling ratio changes with the temperature are shown in Fig. 4. Clearly, they had the same trend with the water uptake results. The CN-SPI membranes possessed low-swelling properties. For example, despite of its high IEC value ( $\sim 2.1 \text{ mequiv g}^{-1}$ ), the swelling ratio of CN-SPI-4 was less than 19% at  $100^\circ\text{C}$ . Lower swelling suggested CN-SPI membranes more competitive for their further applications.

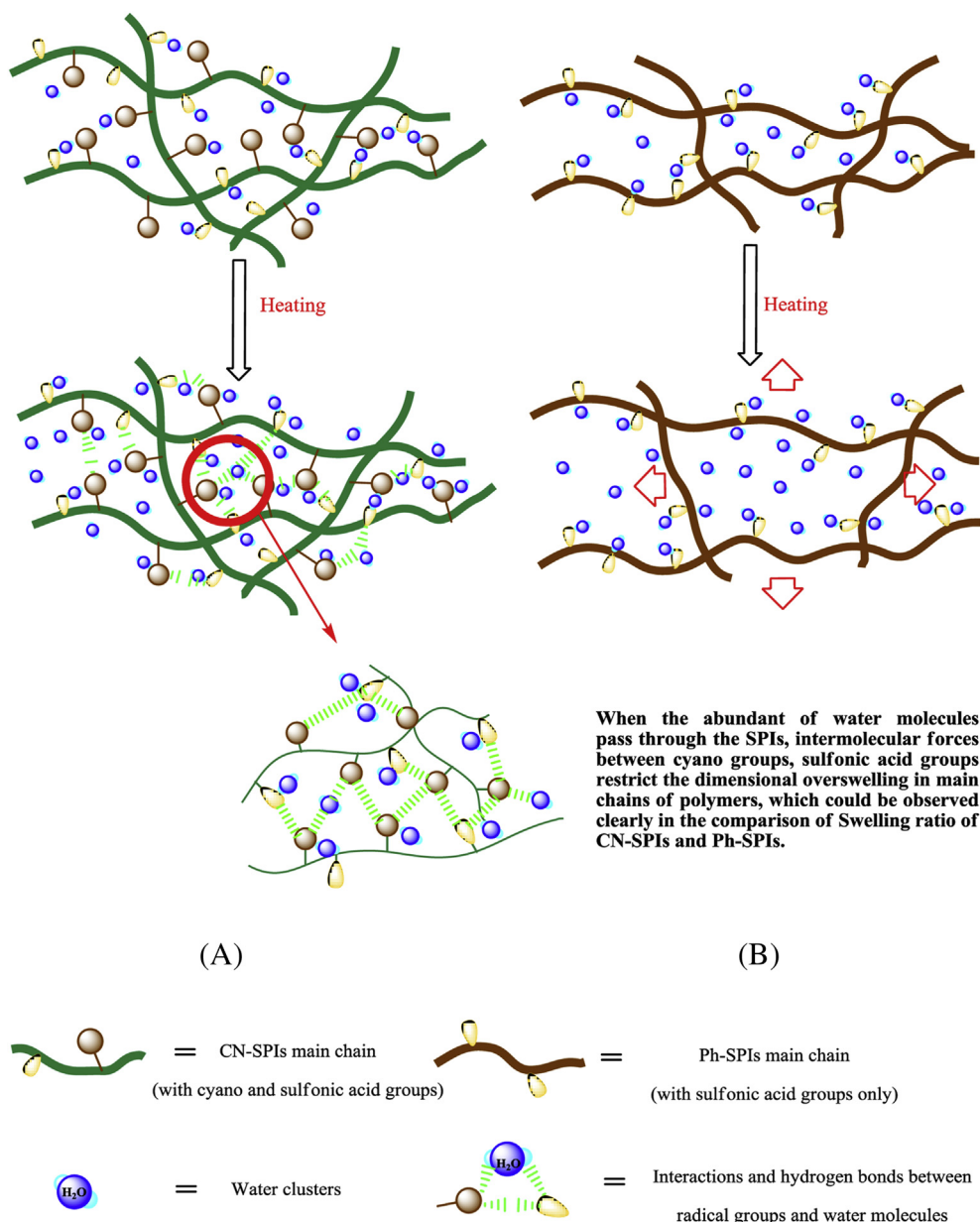


Fig. 6. Water absorption and dimensional change illustration of CN-SPIs (A) and Ph-SPIs (B).

A direct comparison of swelling between CN-SPIs and Ph-SPIs is shown in Fig. 5. Obviously, at each of the IEC, CN-SPIs had better dimensional stability than Ph-SPIs at both 80 °C and 100 °C. In addition, judging from the slopes in the plots, which indicated the rate of the dimensional change with the IEC values, Ph-SPIs were more sensitive to the IEC values. To better illustrate the function of multi-cyano groups, a schematic illustration is given in Fig. 6. Because the strong intermolecular forces, which are called dipole–dipole forces between polar molecules such as cyano groups and sulfonic acid groups, existed in CN-SPIs, the dimensional over-swelling of the CN-SPI membranes was restricted. It well explained why the CN-SPI had better dimensional stability under the circumstance of high humidity and high temperature.

### 3.3. Thermal and oxidative stability of membranes

Thermal properties of CN-SPIs and Ph-SPIs were studied by DSC and TGA measurements, and the results are listed in Table 3. The glass transitions were not clearly observed possibly because of the strong interactions of ionic groups. TGA results showed that the 5% weight loss temperature was above 357 °C and the 10% weight loss temperature was above 413 °C. As shown in Fig. 7, there were two distinct weight loss steps in the TGA curves. The first step was caused by the loss of sulfonic acid groups, and the second step was attributed to decomposition of the main chain of polymers. No obvious difference in the thermal stability of CN-SPIs and Ph-SPIs was observed. The results suggested that all the membranes had good thermal stability (Table 1).

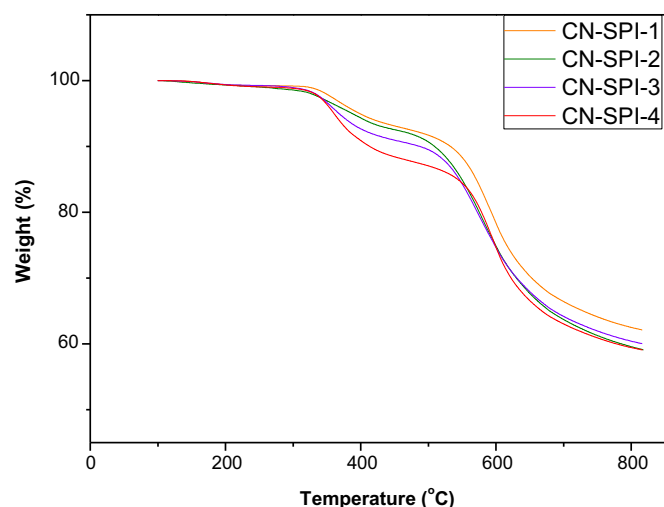
Oxidative stability is one of the important parameters for the PEMs to be applied in fuel cells. The oxidative stability of the membranes was evaluated by observing their dissolving behavior in Fenton's Reagent at 80 °C. After treating in Fenton's Reagent for 1 h, the remaining weights of all the CN-SPI samples were above 99%. Except that Ph-SPI-4, all the other samples stayed integrated in Fenton's reagent for over 10 h at 80 °C. CN-SPI-4 with IEC 2.1 mequiv g<sup>-1</sup> films also exhibited good stability in oxidative resistance.

### 3.4. Mechanical properties of membranes

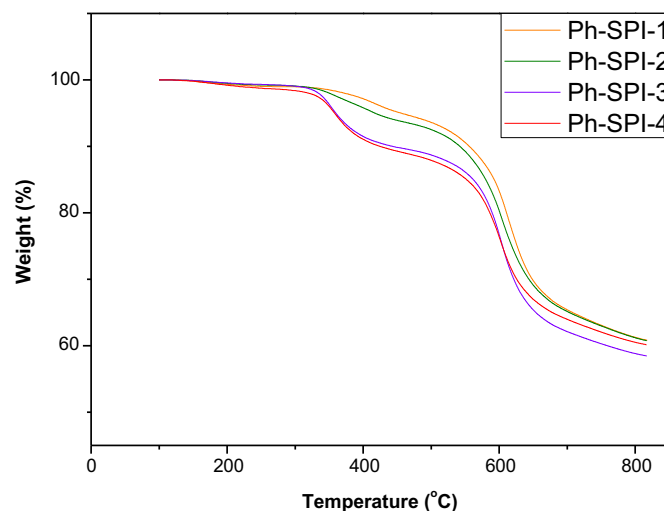
Good mechanical properties are required for the usage of the PEMs. Tensile results in both dry and wet conditions are tabulated in Table 3. Both series of membranes had good tensile properties, and CN-SPIs membranes showed better mechanical properties in both tensile strength and elongation. For example, CN-SPIs membranes exhibited tensile strengths in the range of 62.7 MPa–70.4 MPa in dry state and 26.4 MPa–37.1 MPa in wet state, which were even higher than those of Ph-SPIs. This may be associated with the string interactions caused by the –CN groups on the CN-SPI backbones. It should be mentioned that these interactions

**Table 3**  
Mechanical properties of membranes.

Polymer	Tensile strength (MPa)		Maximum elongation (%)		Young's modulus (GPa)	
	Dry	Wet	Dry	Wet	Dry	Wet
CN-SPI-1	67.6	37.1	17.6	18.1	1.25	0.98
CN-SPI-2	62.7	35.9	15.6	16.5	1.19	0.93
CN-SPI-3	70.4	31.9	22.4	22.7	0.58	0.55
CN-SPI-4	63.7	26.4	20.8	21.4	0.78	0.55
Ph-SPI-1	50.9	26.6	9.11	9.6	0.74	0.82
Ph-SPI-2	44.1	31.1	11.9	14.2	1.06	0.38
Ph-SPI-3	57.7	22.6	14.8	16.5	1.09	0.76
Ph-SPI-4	50.4	17.7	15.6	15.9	1.24	0.74



(A)



(B)

Fig. 7. TGA curves of CN-SPI (A) and Ph-SPI (B).

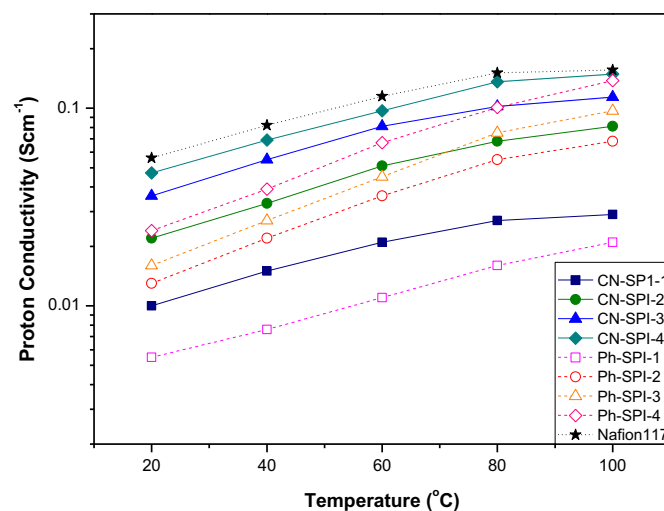


Fig. 8. Proton conductivity of the membranes.

**Table 4**  
Methanol diffusion, selectivity and oxidative stability of membranes.

Polymer	Methanol diffusion ( $\times 10^{-7}$ cm <sup>2</sup> s <sup>-1</sup> )	Selectivity ( $\times 10^5$ S scm <sup>-3</sup> )	Proton conductivity at 100 °C (S cm <sup>-1</sup> )	Oxidative stability RW (%) <sup>a</sup>	t (h) <sup>b</sup>
CN-SPI-1	1.77	1.64	0.029	99.7	>15
CN-SPI-2	3.74	2.17	0.081	99.5	>12
CN-SPI-3	4.91	2.32	0.114	99.6	>10
CN-SPI-4	5.82	2.56	0.149	99.1	>10
Ph-SPI-1	1.74	1.21	0.021	99.8	>11
Ph-SPI-2	3.09	2.19	0.068	99.2	>10
Ph-SPI-3	3.81	2.54	0.097	99.1	>10
Ph-SPI-4	4.25	3.25	0.138	98.2	>8
Nafion117	28.6	0.55	0.156	—	—

<sup>a</sup> Remaining weight after treating in Fenton's Reagent for 1 h.

<sup>b</sup> Dissolved time of membranes.

could even be proved by the strong adhesive forces when the CN-SPI membranes were peeled from the plates at the stage of membrane making.

### 3.5. Proton conductivity, methanol permeability and selectivity of membranes

Proton conductivity and methanol permeability are two dominant transport properties which directly determine the fuel cell performances. High proton conductivity and low methanol diffusion were required as ideal properties for direct methanol fuel cells (DMFCs) [1,3]. The proton conductivity of membranes was estimated using impedance diagrams, and the results are shown in Fig. 8. Generally, the proton conductivity of membranes increased with the test temperature, which was in accordance with the most reported results based on sulfonated polyaromatic membranes. Except that the low IEC samples (Ph-SPI-1 and CN-SPI-1), the proton conductivity at room temperature was much higher than 0.01 S cm<sup>-1</sup>. At 100 °C, the proton conductivity of CN-SPI-4 and Ph-SPI-4 could reach to around 0.14 S cm<sup>-1</sup>, which was quite close to that of Nafion. In addition, some interesting phenomena could be observed. Firstly, CN-SPIs showed similar changing trends with Nafion. Secondly, CN-SPIs had higher conductivity in the low temperature zones. Thirdly, the conductivity of Ph-SPIs increased faster than that of CN-SPIs especially at high temperature. All of these could be in agreement with their water uptake and dimensional swelling behaviors, as depicted above.

The methanol diffusion coefficients of the membranes were in the range of  $1.74 \times 10^{-7}$ – $5.82 \times 10^{-7}$  cm<sup>2</sup> s<sup>-1</sup>, which were much lower than that of Nafion 117 ( $28.6 \times 10^{-7}$  cm<sup>2</sup> s<sup>-1</sup>), as shown in Table 4. In order to well evaluate the combined effect of proton conductivity and methanol crossover, selectivity calculated by using the ratio of proton conductivity (at 100 °C) versus methanol permeability was given (Table 4). The results showed the selectivity of membranes were one order magnitude higher than that of Nafion 117. CN-SPI-4 and Ph-SPI-4 had the best results in their own series.

## 4. Conclusions

A new family of multiple cyano groups-containing sulfonated polyimides (CN-SPIs) were synthesized for the first time. Meanwhile, some similar SPIs but without cyano groups (Ph-SPIs) are prepared as counterparts. After carefully comparing the properties of CN-SPIs and Ph-SPIs, some positive effects of the –CN groups on

the properties were found. Generally, both series of membranes could have good thermal and oxidative stability, acceptable tensile properties, high proton conductivity and low methanol permeability. In compared with Ph-SPI membranes, CN-SPI membranes exhibited better dimensional stability especially at high temperature, which could be explained by the strong interactions mainly caused by –CN groups. The changes in proton conductivity with test temperature could be well explained with their water uptake behaviors. At 100 °C, the CN-SPI-4 showed high proton conductivity comparative to Nafion 117, while its methanol diffusion was much lower. The results showed the CN-containing polymers can be the promising PEM materials.

## Acknowledgements

Financial support for this project was provided by the National Natural Science Foundation of China (No.: 50973040) and the Science and Technology Development Plan of Jilin Province, China (No.: 20100706), the Scientific Research Foundation for the Returned Overseas Chinese Scholars, State Education Ministry (No.: 504 3C1116801412) and Industrial Technology Research and Development Funds of Jilin Province (No.: 2011004-1).

## References

- [1] M.A. Hickner, H. Ghassemi, Y.S. Kim, B.R. Einsla, J.E. McGrath, *Chem. Rev.* 104 (2004) 4587–4612.
- [2] N. Asano, M. Aoki, S. Suzuki, K. Miyatake, H. Uchida, M. Watanabe, *J. Am. Chem. Soc.* 128 (2006) 1762–1769.
- [3] B. Liu, G. Robertson, D. Kim, M. Guiver, W. Hu, Z. Jiang, *Macromolecules* 40 (2007) 1934–1944.
- [4] B.C.H. Steele, A. Heinzel, *Nature* 414 (2001) 345–352.
- [5] M. Rikukawa, K. Sanui, *Prog. Polym. Sci.* 25 (2000) 1463–1502.
- [6] T. Higashihara, K. Matsumoto, M. Ueda, *Polymer* 50 (2009) 5341–5357.
- [7] K. Miyatake, H. Zhou, H. Uchida, M. Watanabe, *Chem. Commun.* (2003) 368–369.
- [8] B.R. Einsla, Y. Hong, Y.S. Kim, F. Wang, N. Gunduz, J.E. McGrath, *J. Polym. Sci. Part A: Polym. Chem.* 42 (2004) 862–874.
- [9] B. Liu, Y. Kim, W. Hu, G. Robertson, B. Pivovar, M. Guiver, *J. Power Sources* 185 (2008) 899–903.
- [10] M. Guo, X. Li, L. Li, Y. Yu, Y. Song, B. Liu, Z. Jiang, *J. Membr. Sci.* 380 (2011) 171–180.
- [11] K. Matsuoka, Y. Iriyama, T. Abe, M. Matsuoka, Z. Ogumi, *J. Power Sources* 150 (2005) 27–31.
- [12] M. Guo, B. Liu, S. Guan, L. Li, C. Liu, Y. Zhang, Z. Jiang, *J. Power Sources* 195 (2010), 4613–4621.
- [13] S. Chen, X. Zhang, K. Chen, N. Endo, M. Higa, K. Okamoto, L. Wang, *J. Power Sources* 196 (2011) 9946–9954.
- [14] X. Zhang, S. Chen, J. Liu, Z. Hu, S. Chen, L. Wang, *J. Membr. Sci.* 371 (2011) 276–285.
- [15] C. Genies, R. Mercier, B. Sillion, N. Cornet, G. Gebel, M. Pineri, *Polymer* 42 (2001) 359–373.
- [16] F. Piroux, R. Mercier, D. Picq, E. Espuche, *Polymer* 45 (2004) 6445–6452.
- [17] K. Miyatake, H. Zhou, M. Watanabe, *Macromolecules* 37 (2004) 4956–4960.
- [18] J. Fang, X. Guo, S. Harada, T. Watari, K. Tanaka, H. Kita, K. Okamoto, *Macromolecules* 35 (2002) 9022–9028.
- [19] N. Asano, M. Aoki, S. Suzuki, K. Miyatake, H. Uchida, M. Watanabe, *J. Am. Chem. Soc.* 35 (2002) 6707–6713.
- [20] B. Liu, W. Hu, G. Robertson, M. Guiver, *J. Mater. Chem.* 18 (2008) 4675–4682.
- [21] P. Xing, G. Robertson, M. Guiver, S. Mikhailenko, S. Kaliaguine, *Macromolecules* 37 (2004) 7960–7967.
- [22] W. Zhang, V. Gogel, K. Friedrich, J. Kerres, *J. Power Sources* 155 (2006) 3–12.
- [23] M. Guo, B. Liu, Z. Liu, L. Wang, Z. Jiang, *J. Power Sources* 189 (2009) 894–901.
- [24] R. Langner, G. Zundel, *J. Phys. Chem.* 99 (1995) 12214–12219.
- [25] M. Sumner, W. Harrison, R. Weyers, Y. Kim, J. McGrath, J. Riffles, A. Brink, M. Brink, *J. Membr. Sci.* 239 (2004) 199–211.
- [26] Y. Gao, G. Robertson, M. Guiver, S. Mikhailenko, X. Li, S. Kaliaguine, *Macromolecules* 38 (2005) 3237–3245.
- [27] K. Sung, P. Huang, C. Zhou, *J. Fluoresc.* 17 (2007) 492–499.
- [28] Y. Zhang, X. Sun, Y. Niu, R. Xu, G. Wang, Z. Jiang, *Polymer* 47 (2006) 1569–1574.
- [29] C. Yang, Y. Su, Y. Chen, *J. Appl. Polym. Sci.* 102 (2006) 4101–4110.